Design of a new test apparatus to simulate the long-term response of a geomembrane beneath a gravel contact

Ali Sabir & Richard W.I. Brachman
GeoEngineering Centre at Queen's-RMC, Queen's University, Kingston, ON

ABSTRACT
A new apparatus was developed to obtain improved estimates of long-term response of geomembrane beneath a single gravel contact, for geomembrane to be used as part of the base liner system in municipal solid waste landfills. A machined probe, mimicking a coarse gravel particle, was manufactured. The apparatus, used in the study, is a steel vessel (60-mm interior diameter, 85-mm high) capable of simulating the ageing of geomembranes under chemical exposure, elevated temperatures and applied force. Results from prototyping trials of a heating system and leakage detection system are documented. The physical boundary conditions imposed on the geomembrane are discussed. The results from the prototype tests for: 1) the physical response of a 1.5-mm thick, high-density polyethylene geomembrane exposed to a high temperature and synthetic leachate and under 700 N of applied force; and 2) the detection of a leak through the punctured geomembrane, are presented.

RÉSUMÉ
Un nouvel appareil a été développé pour obtenir de meilleures estimations de la réponse à long terme de la géomembrane sous un seul contact de gravier, lorsque géomembrane a été utilisé dans le cadre du système d'étanchéité dans les décharges de déchets solides municipaux. Une sonde usinée, mimant une particule de gravier grossier, a été fabriqué. L'appareil, utilisé dans l'étude, est une cuve en acier (60-mm de diamètre intérieur, 85-mm de hauteur) capable de simuler le vieillissement des géomembranes sous exposition aux produits chimiques, des températures élevées et de la force appliquée. Les résultats des essais de prototypage d'un système de chauffage et système de détection des fuites sont documentés. Les conditions aux limites physiques imposées à la géomembrane sont discutées. Les résultats des tests de prototype pour: 1) la réponse physique de 1,5 mm d'épaisseur, géomembrane en polyéthylène haute densité exposés à une température élevée et de lixiviat synthétique et moins de 700 N de la force appliquée, et 2) la détection d'une fuite à travers la géomembrane perforé, sont présentés.

1 INTRODUCTION

High-density polyethylene (HDPE) geomembranes are commonly used with a low permeable layer like a compacted clay liner to act as a composite liner at the base of landfills. HDPE geomembranes are most typically used in these applications because of their excellent resistance to a wide range of chemicals (e.g., see Tisinger et al. 1991; Koerner 1998; Rowe et al. 2004).

For large landfills, the geomembrane liner may be required to retain contaminants for hundreds of years (Rowe et al. 2004). These composite liners provide an excellent hydraulic barrier provided there are no holes present in the geomembrane. Holes in the geomembrane can arise from damage during installation, loading of the liner and possibly from rupture under long-term tensions induced by overlying gravel drainage materials. These holes can lead to fluid movement through the composite liner. To safeguard the geomembrane against puncture and to limit the long-term geomembrane strains, protection is required. In North America, the method developed by Narejo et al. (1996) is often used to select a protection geotextile based on its ability to prevent puncture of the geomembrane for various conditions (e.g., gravel size, overburden stresses, etc.).

In previous studies (Tognon et al. 2000; Gudina and Brachman 2006; Dickinson and Brachman 2008; Brachman and Gudina 2008) tests were carried out with nominal 50 mm coarse gravel (GP50), a nonwoven needle-punched geomembrane protection, designed against puncture as per Narejo et al. (1996), overlying a 1.5 mm thick high-density polyethylene geomembrane on top of a compacted clay liner and/or geosynthetic clay liner. For test times varying between 10 and 100 h at 250 kPa of applied stress it was reported that no puncture was observed, but the short-term strain in the geomembrane exceeded the allowable geomembrane strain limits (e.g., 3% proposed by Seeger and Müller 2003; 6-8% proposed by Peggs et al. 2005) in the literature. Currently, the potential implication of these large sustained tensile strains on the long-term performance of the geomembrane when beneath a gravel contact is not known.

2 SINGLE POINT INDENTATION TEST CELL

A new test cell was designed taking into consideration that the tests are to be carried out at different temperatures, relatively long-time and with leachate on top. To obtain consistent results across the test regime, a steel probe was designed to impart average geomembrane strains for a 50-mm gravel particle. The

test cell is shown in Figure 2. The apparatus had an inside diameter of 60 mm and height of 85 mm.

Force was applied to the geomembrane using a steel probe that was machined to simulate a coarse gravel particle. The largest diameter of the probe was 28 mm and narrowed to a point where it touched the geomembrane, as dimensioned in Figure 2. This geometry was selected to mimic the shape of a point gravel contact from nominal 50 mm coarse gravel as defined by Brachman and Gudina (2008). They showed that point contacts were more likely to produce the largest tensile strains in the geomembrane relative to the four other contact types identified. Use of a single machined steel probe rather than real gravel is advantageous to quantify the effects of time and temperature on geomembrane strain under controlled experimental conditions. Also, since the purpose of these tests is to study the time and temperature effects on geomembrane strain from coarse gravel sized particles, the steel probe differs from the one typically used to assess short-term geomembrane puncture in the truncated cone index test (ASTM D5334).

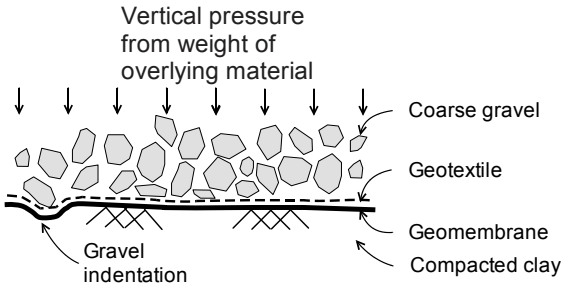

Figure 1. Illustration of gravel contacts leading to local indentations in a geomembrane at the base of a solid waste landfill

3 PHYSICAL BOUNDARY CONDITIONS

The diameter of the test specimen (inside the apparatus) was selected to be 60 mm as this was found to be the mean centre-to-centre spacing between gravel contacts for nominal 50 mm coarse gravel in contact with the geomembrane (Brachman and Gudina 2008).

The geomembrane was mechanically clamped between grooved steel flanges to get a zero radial and zero vertical displacement boundary around the perimeter of the test specimen. The zero radial displacement boundary simulates the situation of multiple equally spaced contact points with the same contact force. The zero vertical displacement boundary produces greater vertical restraint than would be expected in the field, which may result in slightly greater tensile strains in the geomembrane in the laboratory idealization.

4 CHEMICAL EXPOSURE

4.1 Leachate Composition

The leachate consists of a surfactant (5 mL/L Igepal CA720) and a trace metal solution (see Rowe and Islam 2009) and has a pH of 6. Rowe and Islam (2009) demonstrated that this simple synthetic-leachate produced similar oxidative induction time depletion rates compared to more complex leachates involving volatile fatty acids and inorganic nutrients.

4.2 Leachate Refreshing

As antioxidants are depleted from the geomembrane, there is a potential that the concentration of antioxidants in the surrounding fluid will increase. This may change the concentration gradient between the geomembrane and surrounding fluid and thereby reducing the rate of outward diffusion of antioxidants from the geomembrane. Therefore, it was decided to refresh the leachate every two weeks in the experiments to prevent the build-up of antioxidants in the leachate. While the leachate in the gravel above the geomembrane will be changed, the antioxidants may still build-up in the protection layer, if provided.

5 HEATING SYSTEM

The single-point indentation test cell have been designed to operate at elevated temperatures of ranging from room temperature to 100°C to permit the extrapolation of the geomembrane strains to lower service temperatures. The design of the test cell also allows to quantify the rupture time of the geomembrane under constant sustained vertical load at elevated temperature and chemical exposure to be recorded.

A heating and insulation system is then required to initially heat the geomembrane and soil materials and then maintain the geomembrane at the test temperature. The heating system consists of heating cables that are wrapped around the perimeter of the body of the cell which are connected to a control system. A BriskHeat® heating cable that is 15-mm wide and 3-mm thick was selected. Trials were conducted to the design insulation system. To further reduce the need for a constant thermal input and to maintain the test temperature, the test cell is also wrapped with insulation. The final design consists of a removable heating jacket with 50-mm-thick fiberglass insulation contained inside a silicone-coated fiberglass cloth.

Prototyping trial was run for 3 100 h to observe whether the temperature can be maintained in the test cell. A schematic of the heating trial is illustrated in Figure 2. A 1.5-mm-thick HDPE geomembrane was placed over compacted clay liner (CCL). The CCL was installed at an initial water content of 16%. Water was used on top of the geomembrane instead of synthetic leachate and was refreshed every 2 weeks to include any possible temperature effects from refreshing the immersion fluid. One thermocouple was used in the soil at the bottom of the CCL (TC-1), TC-2 was placed at the bottom on the outside of the cell to record the heat loss through the

bottom of the cell, eight thermocouples were used to measure the temperature on the geomembrane (TC-3-TC-10). TC-11 was located on the top of the cell while TC-12, TC-13 and TC-14 were located on the load frame. The last thermocouple, TC-15, was located on the table where the load frame was placed.

Table 1 provides the location of 15 thermocouples used in the study. While temperature recorded at the these 15 points once steady-state thermal conditions were attained for the particular set-point temperature of 85°C are given in Table 2. Table 2 also provided the maximum, minimum, mean and standard deviation of the data. The data given in Table 2 is from the prototype test run for 3 100 h. Figure 3 present the temperature profile for the thermocouples present on the top of the geomembrane (TC-3 to TC-6) while Figure 4 records the temperature data for the thermocouples present on the bottom of the geomembrane (TC-7 to TC-10).

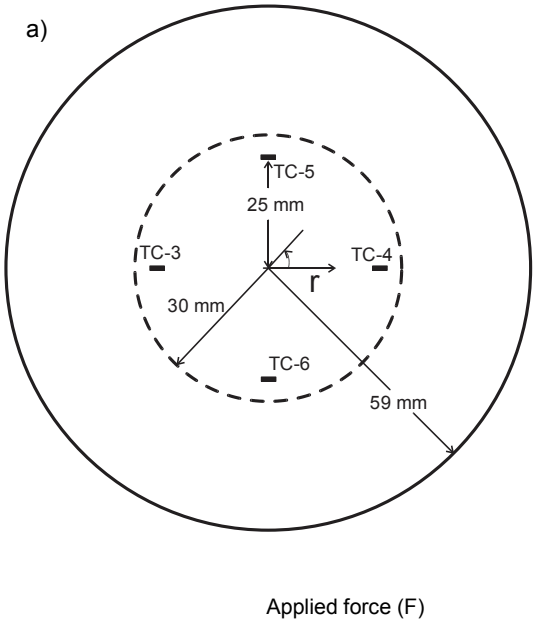

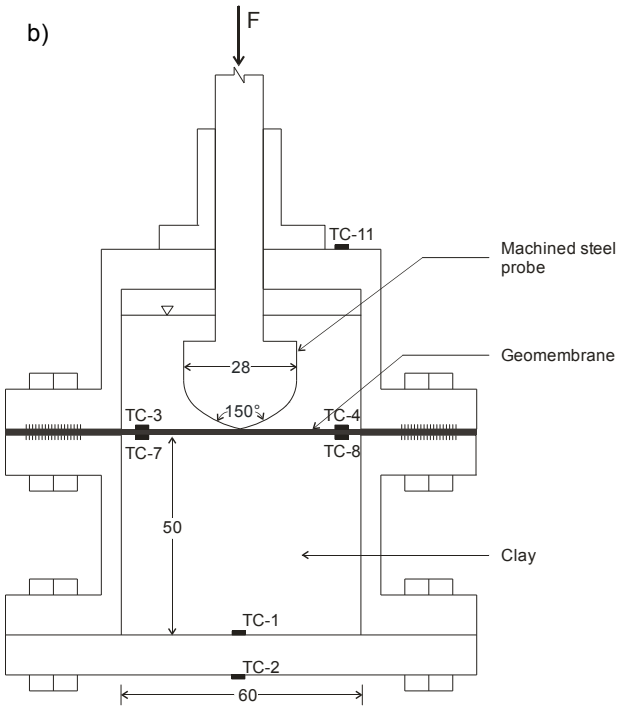

Figure 2. Test cell a) Plan view showing the placement of thermocouples (TC-1 to TC-11); b) Cross section through the test cell (All dimensions in mm)

Once steady-state thermal conditions were reached, the maximum variation of temperature on the geomembrane was ±0.5°C. This demonstrates that the heating system, insulation and controls used for the present study are able to provide control of geomembrane temperatures within ±1°C. The vertical temperature gradient across the geomembrane (across the thermocouples placed on top and bottom of the geomembrane) is small e.g. the difference between the mean temperature for TC-5 and TC-9 was only 0.2°C. This small difference shows that the vertical temperature gradient across the geomembrane was negligible.

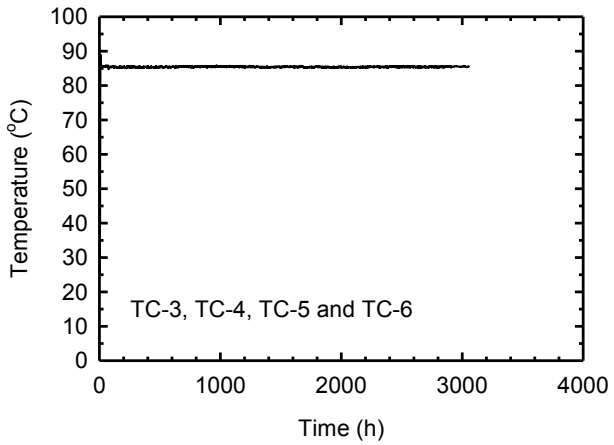

Figure 3. Recorded temperature data for thermocouples placed on top of the geomembrane

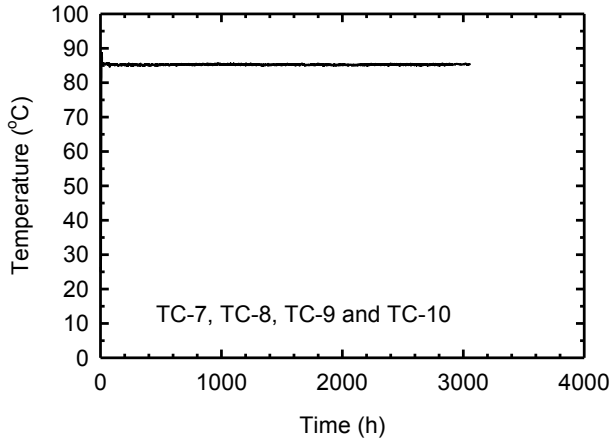

Figure 4. Recorded temperature data for thermocouples placed on the bottom of the geomembrane

Table 3 shows the results from the tests run at 35, 55, 70 and 85°C. The recorded data shows that the heating equipment used in the study is able to maintain the geomembrane temperature within 1°C of the set temperature at all times during the test.

6 LEAKAGE DETECTION SYSTEM

Since tests are also planned that may run until the geomembrane ruptured, a leak detection system was required that can indicate when leakage occurred without the need to visually inspect the geomembrane by physically terminating the test. The leak detection techniques for detecting holes in a geomembrane are well documented (Peggs 1990; Darilek et al. 1989; Laine et al. 1993; Rollin et al. 2002) and several standards have also been developed (ASTM D6747-04; ASTM D7002-03; ASTM D7007). All of these techniques rely on the high electrical resistance of the geomembrane. The intact geomembrane inhibits electrical current between a source electrode above the liner and a receptor electrode beneath the liner. When the geomembrane ruptures, a conduit between the electrodes is established this completes the circuit and can be recorded using a data logging system.

Table 1. Location of thermocouples used in prototype test

Thermo-couple	Location r (mm)	θ (°)	Comment
TC-1			Bottom outside of the cell
TC-2			Bottom inside of the cell
TC-3	25	0	
TC-4	25	90	
TC-5	25	180	
TC-6	25	270	
TC-7	25	0	
TC-8	25	90	
TC-9	25	180	
TC-10	25	270	
TC-11	25	0	Top of the cell
TC-12			Load frame – top
TC-13			Load frame – bottom
TC-14			Load frame – behind the cell
TC-15			Table top

Figure 5 shows the prototype for the leakage detection system. The side walls of the cell used in the present study are made of steel that has a very low resistance to electricity therefore even with an intact geomembrane the electrical current could short-circuit around the geomembrane via the mechanical grip, thus giving a false indication of leakage. Therefore, the geomembrane had to be electrically insulated to prevent the electricity from contacting the cell wall. At the same time, to preserve the indentations in the geomembrane, due to applied load, a lead sheet was placed underneath the geomembrane, which also exhibit low electric resistivity. The lead sheet was 0.4 mm thick and 55 mm in diameter. The diameter of the lead sheet was slightly smaller than the internal diameter of the cell (60 mm) so that the lead sheet did not come in contact with the side walls. To further insulate the geomembrane and lead sheet, a thin plastic sheet 55 mm in diameter, was placed underneath the lead sheet such that there was no direct contact between the compacted clay and the lead sheet. The plastic sheet did not touch the cell walls therefore did not impact the gripping of the geomembrane in the mechanical grip of the cell.

Table 2. Recorded temperature for the prototype test run for 3 100 h

Thermocouple	Temperature (°C)			
	Max.	Min.	Mean	Std. Dev
TC-1	87.7	82.5	83.1	0.6
TC-2	92.7	83.7	84.9	0.7
TC-3	85.7	84.7	85.2	0.2
TC-4	85.6	83.2	84.6	0.2
TC-5	85.2	84.2	84.9	0.2
TC-6	85.7	83.4	84.7	0.2
TC-7	85.5	84.5	85.2	0.2
TC-8	85.4	83.0	84.4	0.2
TC-9	85.2	84.0	84.7	0.2
TC-10	85.4	83.2	84.6	0.2
TC-11	26	23.6	24.6	0.5

TC-12	30.0	25.6	27.7	0.8
TC-13	23.8	21.1	22.4	0.5
TC-14	21.5	17.3	19.4	0.5
TC-15	22.4	18.5	20.8	0.6

Table 3. Recorded temperature (^{o}C) for tests run for 1 000 h at various test temperatures

Set Temperature	Maximum	Minimum	Mean	Standard deviation
35	36.3	34.5	35.2	0.2
55	55.6	54.2	54.9	0.2
70	70.8	69.1	69.7	0.2
85	85.5	84.1	84.8	0.1

Synthetic leachate was placed on top of the geomembrane with a depth of 30 mm and an electrode was placed in the leachate which exited the cell via a port on the top (Figure 5). The lead sheet that was installed beneath the geomembrane was connected to an electrode, which exited the cell through a side port. A 5 volt power supply was connected to the circuit and the resulting voltage was measured with data acquisition software. The circuit was set up so that when no current was able to pass between the electrodes the voltage reading was maximum i.e., 5 volts. When the geomembrane was ruptured and the current was able to pass between the electrodes the voltage reading drops and the test was terminated. The prototype test was run at a deformation rate of 1 mm/min. As the geomembrane ruptured the voltage dropped across the geomembrane. The result from one prototype test is shown in Figure 6.

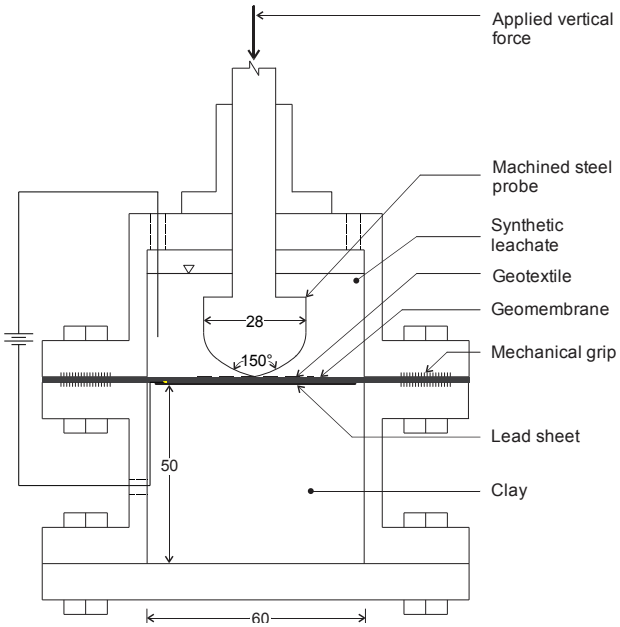

Figure 5. Cross section through the test cell showing the leakage detection system (All dimensions in mm)

7 PRELIMINARY RESULTS

7.1 Deformations

Typical time-displacement curves from the two preliminary tests at maximum applied force of 700 N, run at test temperature of 22 and 55°C with no protection layer is shown in Figure 7. The results show the loading response which was a rapid increase in displacement followed by a small increase with time. The displacements measured at 60 h increased with increasing temperature. The displacement results for times greater than 60 h show the increase in displacement from creep when the applied force was held constant.

Deformed geomembrane shapes for the tests run at 22 and 55°C with no protection layer are compared in Figure 8. Here *v* is the vertical displacement measured from the initial top surface of the geomembrane. It was observed that the indentations in the geomembrane became deeper with an increase in temperature at a given time.

These experiments provided the response of the system (i.e., clay and geomembrane) to time and temperature at a maximum applied force of 700 N. It can be argued that it is the performance of the system that will influence the long-term performance of the geomembrane in landfill applications.

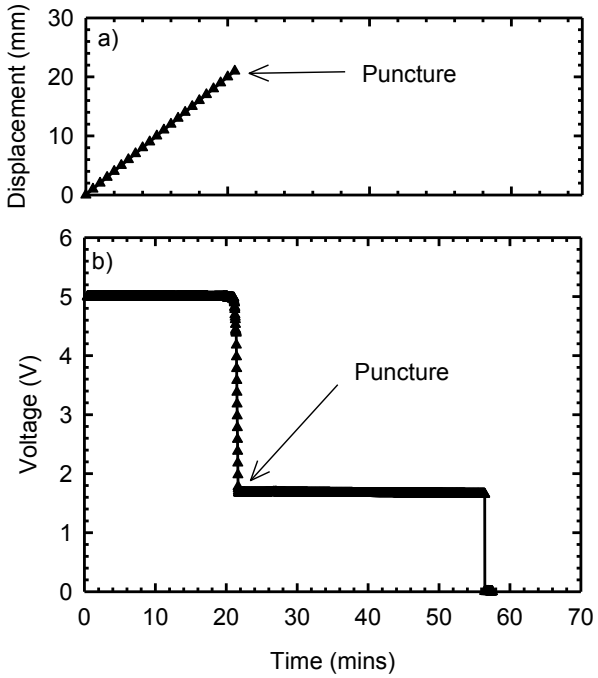

Figure 6. Result from prototype test for leakage detection system showing a) probe displacement with time and b) voltage reading with time

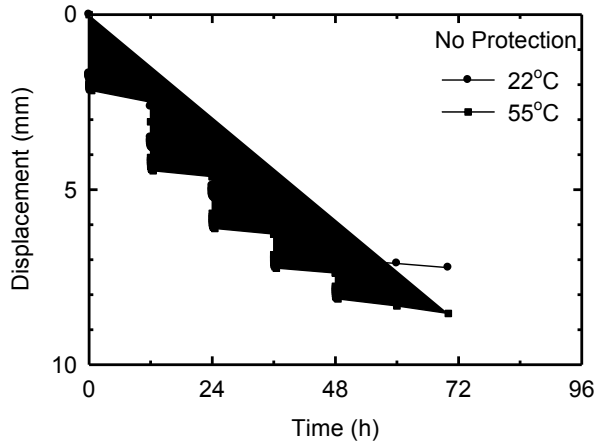

Figure 7. Load-time deflection curves for tests conducted at 22 and 55°C

7.2 Geomembrane Strains

The quantity of practical interest, i.e., geomembrane strain, was calculated from each measured deformed shape using the method developed by Tognon et al. (2000). Result for the tests conducted at 22 and 55°C for the tests are shown in Figure 9a and 10a respectively. The computed strains for the respective indentations are shown in Figure 9b and 10b for the top and bottom surface of the geomembrane. Tensile strains are taken as positive. In both the tests the largest tensile strain occurred on the bottom surface located roughly half-way up the indentation (i.e., approximately 12 mm away from the deepest point) as a result of membrane strain combined with some bending. As the indentation due to the applied force develops, the material on the side of the slope elongates which results in tensile strain. When the indentation is deeper and narrower, the elongation tends to be larger, resulting in higher tensile strains. The maximum strain in all the tests carried out in this study occurred along the side slope of the indentation.

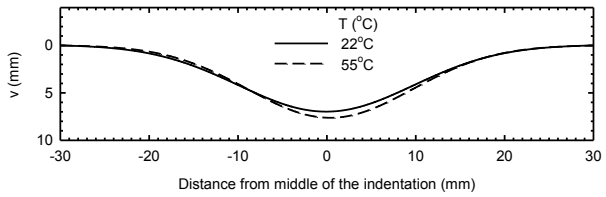

Figure 8. Comparison of the deformed geomembrane shape with no protection for tests run at 22 and 55°C

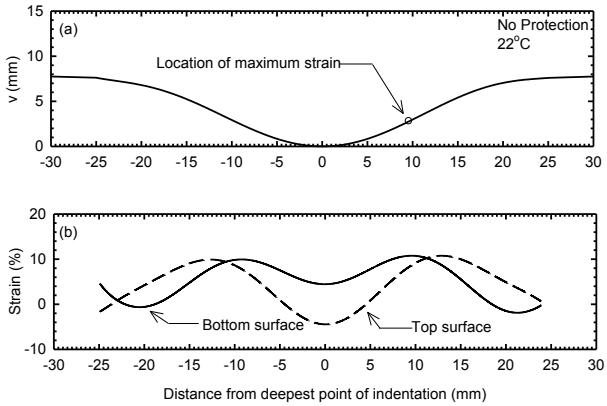

Figure 9. a) Measured geomembrane indentation and b) calculated geomembrane strains for tests at 22°C

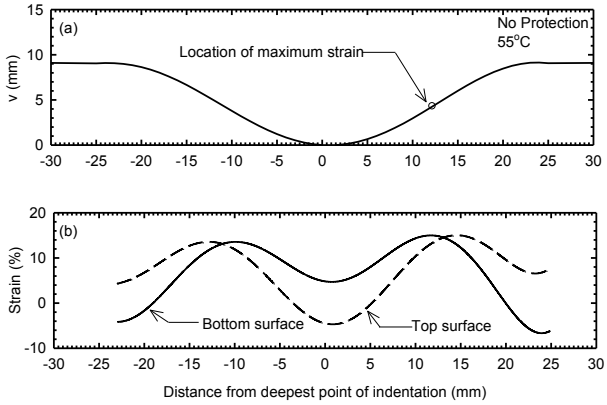

Figure 10. a) Measured geomembrane indentation and b) calculated geomembrane strains for tests at 55°C

The initial results for the influence of temperature on the calculated geomembrane strains for tests conducted at an applied force of 700 N (for a test time of 10 h) show that the difference in geomembrane strain can be attributed to the change in the test temperature. The geomembrane strains increase by approximately 1.4 times as the temperature increased from 22°C to 55°C for the tests conducted for 10 h duration. It is has been shown (Ferry 1980) that at higher temperatures, the modulus of the geomembrane decreases thereby increasing the creep of the material. This increase in the material creep may result in increased indentation depth and, consequently, larger geomembrane strains at longer times.

8 SUMMARY

The development of a new experimental apparatus that is capable of simulating the ageing of geomembranes under the combined effects of chemical exposure, elevated temperatures and applied stresses was described. Results from prototyping trials of a temperature insulation show that the heating and insulation systems developed are able to provide control of geomembrane temperatures within ±1°C for the set point of 85°C. Details of a leachate

detection system were presented. Two initial tests performed using the cell were presented to quantify the increase in geomembrane strains that increased by a factor of 1.4 with an increase in temperature from 20 to 55°C for tests than ran for 58 h. Experiments are currently underway to provide improved estimates of the geomembrane strains under sustained vertical loading at various temperatures and temperatures.

REFERENCES

American Society for Testing and Materials. 2007e. Standard guide for selection of techniques for electrical detection of potential leak paths in geomembrane (D6747). In annual book of ASTM standards. Vol. 04.13. American Society for Testing and Materials, Philadelphia, Pa

American Society for Testing and Materials. 2007f. Standard practice for leak location on exposed geomembranes using the water puddle system (D7002-03). In annual book of ASTM standards. Vol. 04.13. American Society for Testing and Materials, Philadelphia, Pa.

American Society for Testing and Materials. 2007g. Standard practices for electrical methods for locating leaks in geomembranes covered with water or earth materials. In annual book of ASTM standards. Vol. 04.13. American Society for Testing and Materials, Philadelphia, Pa.

Brachman, R.W.I., and Gudina, S. 2008. Gravel contacts and geomembrane strains for a GM/CCL composite liner. Geotextiles and Geomembranes 26 (6), pp448–459.

Darilek, G.T., Laine, D. L., and Porra, J.O. 1989. The electric leak location method for geomembrane liners, In Proc. Geosynthetics '89, San Diego, CA, IFAI Publ., pp456-66.

Dickinson, S., and Brachman, R.W.I. 2008. Assessment of alternative protection layers for a geomembrane / geosynthetic clay liner (GM/GCL) composite liner. Canadian Geotechnical Journal 45 (11), pp1594–1610.

Ferry, J.D. 1980. Viscoelastic properties of polymers. John Wiley and Sons, New York, pp641

Gudina, S. 2007. Short-term Physical Response of HDPE Geomembranes from Gravel Indentations and Wrinkles. PhD thesis, Department of Civil Engineering, Queen's University, Kingston, Ontario.

Gudina, S. and Brachman, R.W.I. 2006. Physical Response of Geomembrane Wrinkles Overlying Compacted Clay, Journal of Geotechnical and Geoenvironmental Engineering, 132(10), pp1346-1353.

Rowe, R.K. and Islam, M.Z. 2009. "Impact on landfill liner time-temperature history on the service-life of HDPE geomembranes", *Waste Management*, 29(10):2689-2699.Koerner, R.M. (1998). Designing with Geosynthetics, 4th ed., Prentice Hall, New Jersey, USA.

Laine, D.L., and Darilek, G.T. 1993. Locating leaks in geomembrane liners of landfills covered with a protective soil. Proceedings of Geosynthetics 1993, Vol 3, pp1403-1412.

Narejo, D., Koerner, R.M., and Wilson-Fahmy, R.F. 1996. Puncture protection of geomembranes, part II: experimental. Geosynthetics International 3(5), pp629–653.

Peggs, I.D., Schmucker, B., and Carey, P. 2005. Assessment of maximum allowable strains in polyethylene and polypropylene geomembranes. In: Geo-Frontiers 2005 (CD-ROM). American Society of Civil Engineers, Reston, VA.

Rollin A.L., Marcotte M., Chaput, L. and Caquel, F. 2002. Lessons learned from geoelectrical leaks surveys, Proccedings of Geosynthetics 2002, Nice, pp527-530.

Rowe, R.K., Quigley, R.M., Brachman, R.W.I., and Booker, J.R. 2004. Barrier systems for waste disposal, 2nd ed., Spon Press, London.

Seeger, S. and Müller, W. 2003. Theoretical approach to designing protection: selecting a geomembrane strain criterion. In: Dixon, N., Smith, D.M., Greenwood, J.H., Jones, D.R.V. (Eds.), Geosynthetics: Protecting the Environment. Thomas Telford, London, pp137–152.

Tisinger, L.G., Peggs, I.D., and Haxo, H.E. (1991). Chemical compatibility testing of geomembranes, Geomembranes Identification and Performance Testing¸ Edited by A.Rollin, and J.M. Rigo, Rilem Report 4, Chapman and Hall, pp. 268-307.

Tognon, A.R., Rowe, R.K., and Moore, I.D. 2000. Geomembrane strain observed in large scale testing of protection layers. ASCE Journal of Geotechnical and Geoenvironmental Engineering 126 (12), pp1194–1208.